

Thermally stratifying a wind tunnel for buoyancy influenced flows

J. H. Lienhard V

Department of Mechanical Engineering, Massachusetts Institute of Technology, Cambridge, MA 02139, USA

C. W. Van Atta

Department of Applied Mechanics and Engineering Sciences, University of California at San Diego, La Jolla, CA 92093, USA

Abstract. A novel method of heating wind tunnel flows to strong thermal stratifications is described. Variable electric heating is employed to create user-selectable temperature profiles in steady, uniform mean flow. Linear temperature gradients of up to $200^{\circ}\text{C}/\text{m}$ (Väisälä frequencies of 2.5 rad s^{-1}) can be sustained. The performance of the facility is discussed in the context of continuously-stratified grid-generated turbulence, although it is useful for a broader set of applications. The flow field is found to be free of deleterious natural convection and internal wave effects. The departure from homogeneity of grid-generated, stratified turbulence in the facility is roughly $\pm 10\%$ away from the wall influenced regions.

1 Introduction

The creation of stratified flows manifesting active buoyancy forces has long posed a challenging experimental problem. To date, only salt-stratified water flows, either tow-tanks or water tunnels, have been able to achieve the high density gradients required to develop dynamically significant buoyancy forces in the laboratory. Of those experiments, only a unique salt-stratified water tunnel facility (Stillinger et al. 1983) has generated reasonably steady flows with significant run times.

The salt-water flows suffer from a variety of instrumentation problems which make detailed statistical data difficult to obtain. Spectral and cross-spectral data, scalar dissipation rates, and long recording times all severely test the limits of current sensors. These concerns, as well as the need to work at other Prandtl numbers, motivate the alternative use of thermally stratified air flows.

Air experiments have to date been confined to wind tunnels with weak temperature gradients for which buoyancy forces were negligible (Wiskind 1962; Montgomery 1974; Venkataramani and Chevray 1978; Sirivat and Warhaft 1983). In part, the absence of previous actively stratified air experiments has resulted from the perception that strongly

stratified temperature profiles will be very difficult to produce. Here, we present a heat exchanger for producing such strong stratifications in a laboratory wind tunnel flow.

The stratified wind tunnel is shown schematically in Fig. 1. Air is driven through the tunnel at overpressure relative to ambient room pressure by a low-turbulence blower upstream¹. It enters a variable electric heat exchanger and shear abatement unit which heats the flow differentially while maintaining a uniform velocity profile. The flow next passes through a 2.5:1, two-dimensional contraction. This contraction effectively increases the stratification by raising the temperature gradient, since the initial temperature difference is imposed across a smaller vertical height. The flow then enters a test-section from which it is exhausted to the room. For decaying turbulence studies, a biplane grid is placed between the contraction and the test-section. For other studies, different obstacles can be used, e.g. a cylinder for stratified wake experiments.

This facility is capable of producing linear stratifications² of up to $200^{\circ}\text{C}/\text{m}$ at uniform mean speeds in the range of 2–5 m/s. However, the discrete heating control is also suitable for the generation of various nonlinear temperature profiles, such as a thermocline profile. The flow field shows good uniformity and homogeneity. In addition, the facility is supercritical to internal waves under normal operating conditions.

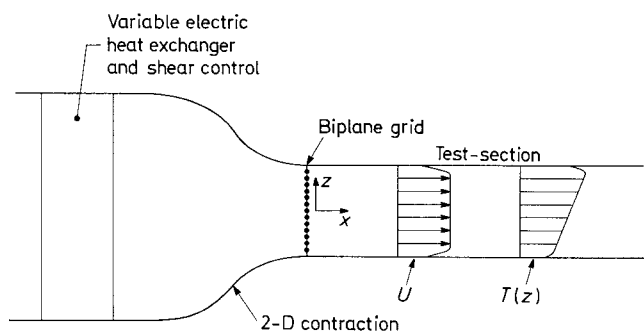


Fig. 1. Heat exchanger, final contraction, and test-section of the thermally stratified wind tunnel

¹ The present test-section was located at the exit of an existing wind tunnel's 10:1 contraction

² Stratification is also characterized by the Brunt-Väisälä frequency, $N = (g/T dT/dz)^{1/2}$. Väisälä frequencies as high as 2.5 rad s^{-1} have been produced with this facility

2 Heat exchanger design

The heat exchanger is a fin-tube crossflow exchanger. The heating elements are electric heater rods which constitute the 'tubes' of the exchanger. The fins are situated transverse to the rods, parallel to the flow direction. The design equations were derived from standard methods of thermal engineering and are not reproduced here (Lienhard 1988). The bases of the design were a model for the convective heat removal from the fins and a desired range of operating speeds and stratifications.

The heat exchanger is shown schematically in Fig. 2. It is triangular, being 0.305 m deep at the top (hot) end and 0.762 m in height and width. Cold air enters at the vertical side of the heater and exits, heated, at the slanted side. The triangular form reflects the general objective of a stable, linear, vertical stratification; the greater depth at the top provides the additional heating surface needed for higher temperatures.

The design uses 45 electric heater rods on a 5.08 by 5.08 cm planform. Each 1 kW heater rod has a nominal heated length of 76 cm, an outer diameter of 8 mm and a maximum operating temperature of 825 °C. The inter-rod spacing and the fin material were chosen to produce fins of a relatively high thermal efficiency (~ 70%), so avoiding large surface temperature gradients which could cause uneven heating.

The triangular fins are made from brass (0.25 mm thick) and are spaced 7.6 mm apart, giving a total of 94 fins across the width of the exchanger. The spacing between the fins is fixed by 4275 brass spacer rings which fit around the heater rods between each fin. The spacers also improve thermal contact between the rods and fins. The heat exchanger is insulated from its supporting frame and environs with asbestos board.

The heater rods are controlled in small groups by variable autotransformers. Electric current, both that available and that allowed by the transformers, was a primary limiting factor on the upper operating temperature of the facility. In principle, however, the heat exchanger can deliver up to 45 kW.

Portions of the vertical sides of the heat exchanger were cold, owing to variations in the actual heated length of the rods. This problem was remedied by reducing the width of the test-section to include only the well-heated portions of the flow. The reduction of cross-section was effected by chopping the flow as it entered the contraction; cool portions were exhausted and warm portions passed into the test-section using a double side-wall arrangement. The working dimensions of the 2-D plywood contraction section were thus a width of 57.8 cm, an inlet height of 76.2 cm, and an outlet height of 30.5 cm.

Table 1 shows how the flow speed and temperature rise relate to the required number of heater rods operating at given power output. (Parameters not varied in the table have the values stated above.) The last column shows the power

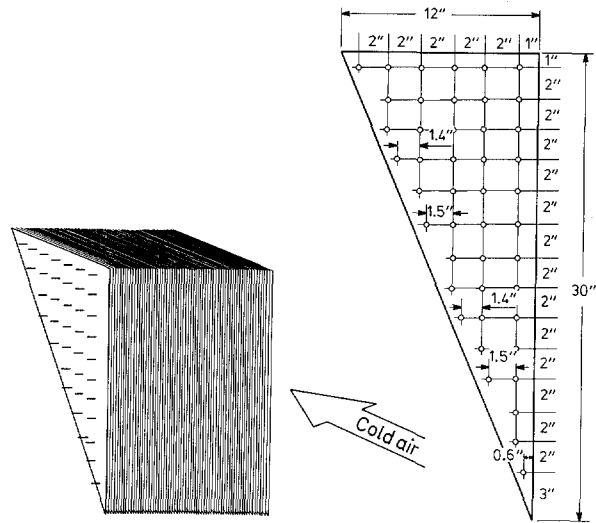


Fig. 2. The heat exchanger

Table 1. Power map: ΔT – air temperature rise through top of exchanger; U – flow speed in test-section; P – total power required; P_r – power to individual rods

ΔT (°C)	U (m/s)	P (kW)	No. of rods			P_r , 45 rods (W)
			300 W	500 W	800 W	
10	2.0	2.70	9	6	4	60
	2.5	3.38	12	7	5	75
	5.0	6.75	23	14	9	150
20	2.0	5.29	18	11	7	118
	2.5	6.61	22	14	9	147
	5.0	13.2	44	27	17	294
40	2.0	10.2	34	21	13	227
	2.5	12.7	43	26	16	282
	5.0	25.4	87	51	32	564
60	2.0	14.6	49	30	19	324
	2.5	18.3	61	37	23	407
	5.0	36.6	122	74	46	813
80	2.0	18.8	63	38	24	418
	2.5	23.5	79	47	30	522
	5.0	47.0	157	94	59	(1044)

output required from the 45 rods actually used for given operating conditions. For most operating conditions, the rods run at less than half of their rated capacity. The choice of 45 rods allows a variety of operating conditions while keeping the individual rods at a fairly low power. The heat exchanger thus remains comparatively cool. The use of higher power for higher flow speed or hotter operating conditions is also possible.

The 7.6 mm fin spacing finally chosen represents a compromise between a higher heat transfer coefficient, obtained as the spacing decreases, and a consequently larger number

of cooler plates. The required 'hot end' length of the heater (in the flow direction) is related to the maximum temperature rise and flow speed at various rod power and fin temperature. The design finally taken used a 30.5 cm depth, biasing the heater toward lower fin temperatures at the operating conditions of interest. The lower temperatures and greater depth are intended to create better temperature uniformity at the outlet.

To prevent shearing the flow, the vertically varying drag of the heat exchanger was balanced by constructing an inverted image of the exchanger plates directly behind the heater, upstream of the contraction. Galvanized steel sheet (0.76 mm thick) was used for the shear control plates; steel is a poor conductor of heat in comparison to the brass used in the heater. To avoid additional turbulent mixing, the shear control was built without the horizontal rods present in the heat exchanger. The shear control unit was made from about 80 plates held by 4 tie rods and separated with 7.6 mm spacers.

The wake of the heater/shear control device most closely resembles a set of channel flows, the channels being formed by the space between adjacent fins. The rods themselves leave no observable structure in either the velocity or temperature fields.

A vertical sheet of plain steel perforated plate (4.0 mm diameter holes, 37% solidity) was placed about 5 cm beyond the shear control plates. The perforated plate removes residual shear and was sized to help destroy the larger scale structures in the wake of the upstream plates. No shear could be measured at the outlet of the contraction.

3 Performance of the heat exchanger

Linear mean temperature profiles were found for a number of Väisälä frequencies and mean speeds of 2.0 m/s and 2.5 m/s. Temperature profiles were set using measurements taken in the test-section itself, without reference to what temperature profile leaving the heater would give the proper profile in the test-section. The settings were established by an iterative measure-and-adjust process.

Typical results, at about 76 cm from the grid, are shown in Fig. 3. The temperature profiles could generally be set so that no point deviated from the linear distribution by more than 0.3°C for the weakly stratified profiles or by more than 1°C for the strongly stratified profiles. The rms error in the mean profiles is considerably smaller. Visually, these profiles are excellent straight lines in the region away from the wall layers. Profiles can be held indefinitely, after an initial first-order warming transient of about one hour.

The flow entering the test-section showed temperature noise of about $\pm 0.36^\circ\text{C}$ at $N=2.1\text{ s}^{-1}$, arising from both the nonuniformity of the heat exchanger and from other upstream mixing processes; this noise was largely on scales below 100 Hz and had no apparent spatial orientation. As a consequence, e.g., in grid-generated turbulence studies the

temperature gradients must be sufficiently large that a given size grid produces initial temperature fluctuations greater than the upstream noise. This requirement was found to limit 2.54 cm mesh grid measurements to stratifications greater than about 1.60 s^{-1} and 5.08 cm mesh measurements to stratifications greater than about 1.16 s^{-1} .

No corresponding noise was observed in the velocity field; velocity fluctuations decay much more rapidly than temperature fluctuations in these flows (Lienhard and Van Atta 1989). The remaining turbulent velocity from the heat exchanger ($u'/U=0.5\%$) was completely eradicated by the grid in every case. However, the streamwise development of θ' for the 5.08 cm grid is less scattered than for the 2.54 cm grid, suggesting that the larger disturbances of the big grid provide a 'cleaner' evolving temperature fluctuation field.

The vertical temperature gradient implies the presence of a vertical heat flux. Once a vertical slab of fluid passes into the test-section, however, no heat input/outflow at the ceiling/floor is present to sustain the profile and it will begin to decay. The behavior of linear temperature profiles in homogeneous turbulence has been discussed by many authors (Corrsin 1952; Wiskind 1962; Montgomery 1974; Venkataramani and Chevray 1978; Sirivat and Warhaft 1983; Lienhard 1988). The essential result is that the temperature profile tends to flatten in diffusion layers near the boundaries, while the central portion of the flow retains its initial linear temperature profile. This behavior is also seen in the present test-section. The profiles show a marked decay near the floor and ceiling, but maintain the initial gradient near the center. The thickness of the diffusion layers is typically commensurate with that of the turbulent wall boundary layers.

The horizontal nonuniformities in the mean temperature are small compared to the level of vertical stratification, and the flow may certainly be viewed as possessing only a uni-

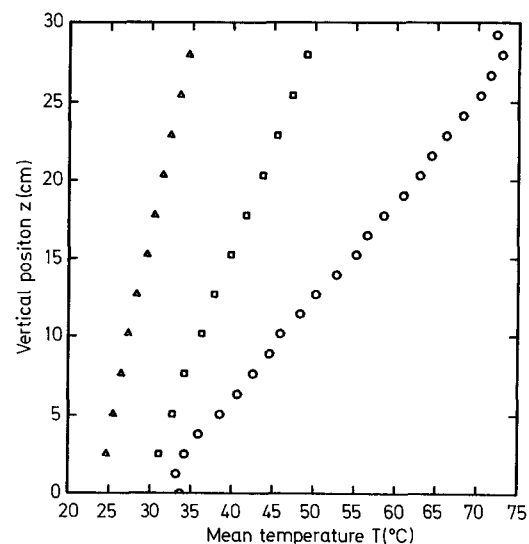


Fig. 3. Typical temperature profiles, $M = 5.08\text{ cm}$: \circ $157^\circ\text{C}/\text{m}$; \square $72.2^\circ\text{C}/\text{m}$; \triangle $41.3^\circ\text{C}/\text{m}$

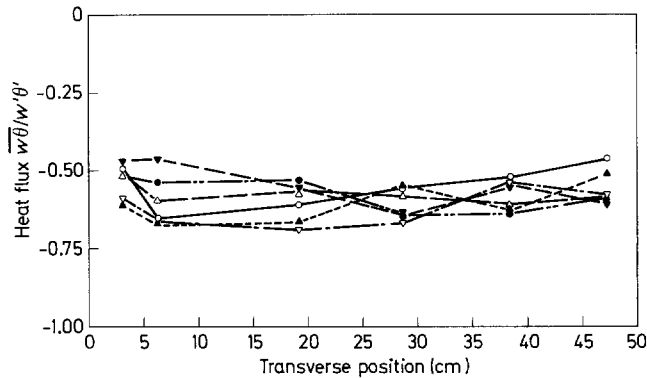


Fig. 4. Profile of the heat flux correlation coefficient; each curve represents a horizontal transverse at a different height

Table 2. Homogeneity of the rms intensities and the correlation coefficients. Definition of % deviation given in text

Quantity	Mean	Std. dev.	% deviation
u'/U	0.0225	0.0014	6.1
w'/U	0.0171	0.0011	6.3
θ'	1.171 °C	0.191 °C	16.0
$w\theta/w'\theta'$	-0.583	0.064	11.0
$\overline{uw}/u'w'$	0.0116	0.0809	10.0

form vertical temperature gradient. No consistent skewing of the temperature profile, which might signal the presence of large-scale natural convection, is present. Measured values of the mean vertical velocity were never greater than 2% of the mean streamwise velocity and were generally positive, which is also inconsistent with any natural convection flow pattern. The measured vertical velocity most likely results from either from slight misalignment of the X-wire or from small errors in the probe calibration.

Another important issue is the question of what sort of internal wave field might be generated within the test-section. Following Turner (1973, §2.3.1), two-dimensional, linear, standing internal waves may be shown to occur only for $Fr_m^2 < 1/\pi^2$, where the internal Froude number is $Fr_m = U/NH$ with H the test-section height and U the mean speed. Since the test flow always has Fr_m greater than about 2.6, it is always supercritical which respect to 2-D standing internal waves. A similar analysis (Lienhard 1988) shows that the passage of the stratified flow through the 2-D contraction should not generate waves unless Fr_m is less than $1/\pi$ upstream of the contraction. The upstream Froude number is always greater than 0.7, so that the flow is also supercritical with respect to these waves. Measurements of the cross-spectral phase (Lienhard and Van Atta 1989) in these flows show no evidence of internal waves in the velocity and temperature field.

3.1 Flow homogeneity in grid turbulence

To test the homogeneity of the flow produced by this heating configuration, a flow mapping experiment was performed for stratified grid turbulence. Measurements of u , w , and θ were made at 36 points in the transverse cross-section at $x/M = 33.8$ for a stratification $N = 2.2 \text{ rad s}^{-1}$, a mean speed of 2.5 m/s, and a 2.54 cm mesh grid (35.7% solidity). The individual time-series were 50 records of 4,096 points at each point sampled (using a sample rate of 2,048 Hz).

The homogeneity of the rms velocity components is characterized by the standard deviation of the intensities, u'/U and w'/U , over the cross-section (Table 2). The spatial distribution of the intensity is homogeneous to 6–9% throughout the wall-independent regions of the test-section. The homogeneity of the rms temperature fluctuation is also shown in Table 2. The rms temperature fluctuation, θ' , is initially homogeneous to an rms deviation of 16% of its spatial average value, and it becomes increasingly homogeneous downstream. The inhomogeneity might be reduced by other types of heaters (such as have been used in the passive case), but seems to be a consequence of designing for high levels of stratification. The spatial variation may also be, in part, a remnant of the relatively small number of records (50) used in the flow mapping experiment.

The rms variation of the convective heat flux correlation coefficient, $w\theta/w'\theta'$, and the Reynolds stress correlation coefficient, $\overline{uw}/u'w'$, are presented as a percentage of the maximum value these correlations might take³. Deviations from homogeneity away from wall influenced regions are about 11% for the heat flux (Fig. 4) and about 10% for the Reynolds stress. The Reynolds stress correlation is essentially zero throughout the core of the test flow, indicating the absence of any mean shear.

A usable core region of the flow retains its basic stratification and homogeneity for more than 4 m downstream, in spite of the growing effects of the wall layers. Further details of the facility, the flow mapping, and the instrumentation are given by Lienhard (1988).

4 Summary

A strongly thermally-stratified, steady-flow wind tunnel has been developed. The facility is capable of producing user selectable temperature profiles; linear profiles up to 200 °C/m are possible at uniform mean velocities in the range of 2–5 m/s. The test-section is supercritical to simple internal wave modes under normal operating conditions. A flow mapping experiment sets the level of homogeneity at roughly 10% for second-order turbulent statistical quantities of interest in grid-generated turbulence. This facility is useful for a wide variety of stratified flow experiments.

3 For the heat flux correlation, this maximum is about 0.6 (Lienhard and Van Atta 1989), and for the Reynolds stress correlation, it is ± 0.4 (the classical shear layer values) which we represent as 0.8.

Acknowledgements

This study was supported by the National Science Foundation under grants no. OCE82-05946 and no. OCE85-11289 with partial support from DARPA under grant no. N00014-86-K-0758.

References

- Corrsin, S. 1952: Heat transfer in isotropic turbulence. *J. Appl. Phys.* 23, 113–118
- Lienhard V, J. H. 1988: The decay of turbulence in thermally stratified flow. Doctoral diss. San Diego: University of California
- Lienhard V, J. H.; Van Atta, C. W. 1989: The decay of turbulence in thermally stratified flow. *J. Fluid Mech.*, in press
- Montgomery, R. D. 1974: An experimental study of grid turbulence in a thermally-stratified flow. Doctoral diss. University of Michigan
- Srivat, A.; Warhaft, Z. 1983: The effect of a passive cross-stream temperature gradient on the evolution of temperature variance and heat flux in grid turbulence. *J. Fluid Mech.* 128, 323–346
- Stillinger, D. C.; Head, M. J.; Helland, K. N.; Van Atta, C. W. 1983: A closed-loop gravity-driven water channel for density-stratified shear flows. *J. Fluid Mech.* 131, 73–89
- Turner, J. S. 1973: Buoyancy effects in fluids. Cambridge: Cambridge University Press
- Venkataramani, K. S.; Chevray, R. 1978: Statistical features of heat transfer in grid-generated turbulence: constant-gradient case. *J. Fluid Mech.* 86, 513–543
- Wiskind, H. K. 1962: A uniform gradient transport experiment. *J. Geophys. Res.* 67, 3033–3048

Received March 14, 1989